Atmospheric Research 200 (2018) 153–168

Contents lists available at ScienceDirect

Atmospheric Research

journal homepage: www.elsevier.com/locate/atmosres

Spatial and temporal analysis of drought variability at several time scales in Syria during 1961–2012

Shifa Mathbout[a,b,*], Joan A. Lopez-Bustins[b], Javier Martin-Vide[b], Joan Bech[a], Fernando S. Rodrigo[c]

[a] Department of Applied Physics-Meteorology, University of Barcelona, Martí i Franquès 1, 08028 Barcelona, Spain
[b] Climatology Group, Department of Geography, University of Barcelona, Montalegre 6, 08001 Barcelona, Spain
[c] Department of Chemistry and Physics, University of Almeria, Spain

ARTICLE INFO

Keywords:
Climate regionalization
Drought
SPEI
SPI
Syrian conflict

ABSTRACT

This paper analyses the observed spatiotemporal characteristics of drought phenomenon in Syria using the Standardised Precipitation Index (SPI) and the Standardised Precipitation Evapotranspiration Index (*SPEI*). Temporal variability of drought is calculated for various time scales (3, 6, 9, 12, and 24 months) for 20 weather stations over the 1961–2012 period. The spatial patterns of drought were identified by applying a Principal Component Analysis (PCA) to the SPI and *SPEI* values at different time scales. The results revealed three heterogeneous and spatially well-defined regions with different temporal evolution of droughts: 1) Northeastern (inland desert); 2) Southern (mountainous landscape); 3) Northwestern (Mediterranean coast). The evolutionary characteristics of drought during 1961–2012 were analysed including spatial and temporal variability of SPI and *SPEI*, the frequency distribution, and the drought duration. The results of the non-parametric Mann–Kendall test applied to the SPI and *SPEI* series indicate prevailing significant negative trends (drought) at all stations. Both drought indices have been correlated both on spatial and temporal scales and they are highly comparable, especially, over a 12 and 24 month accumulation period. We concluded that the temporal and spatial characteristics of the SPI and *SPEI* can be used for developing a drought intensity - areal extent - and frequency curve that assesses the variability of regional droughts in Syria. The analysis of both indices suggests that all three regions had a severe drought in the 1990s, which had never been observed before in the country. Furthermore, the 2007–2010 drought was the driest period in the instrumental record, happening just before the onset of the recent conflict in Syria.

1. Introduction

Drought is one of the most complicated and recurring natural hazards which has different impacts on ecological, economic, social, agricultural, cultural and political areas in almost all climatic regions especially in rain-fed agricultural regions (Kastopoulou et al., 2017; Surendran et al., 2017) with varying frequency, severity and duration (Van Loon, 2015; Deo and Sahin, 2015; Deo et al., 2017). Precipitation is a major parameter for studying hydrological and meteorological variables (Lo Conti et al., 2014; Wang et al., 2016), managing water resources (Retalis et al., 2016; Awchi and Kalyana, 2017) and detecting some natural hazards as drought (Zambrano et al., 2017).

Drought can be characterized in multiple ways (Heim, 2002; Keyantash and Dracup, 2002) and can be defined as a natural recurrent feature of the climate cycle occurring in different climatic zones which is generally perceived to be a prolonged period with significantly lower precipitation relative to normal levels or increased evaporative demand or a combination of both of them. It is a three dimensional complex natural hazard characterized by severity (magnitude or intensity), duration and areal extent (Tsakiris et al., 2007; Vicente-Serrano et al., 2010a, 2012; Mohammed and Scholz, 2017) which may be studied from the environmental or the water resource point of view (Wilhite and Glantz, 1985). The observed impact of climate system changes on droughts varies regionally, based on changes of the drought drivers such as precipitation and temperature and on regional features of the hydro-climate modelling system (Sheffield and Wood, 2008; McCabe and Wolock, 2015). Based on the nature of the water deficit, four types of droughts are defined: meteorological, hydrological, agricultural and socio-economical (Wilhite and Glantz, 1985; Martín Vide and Olcina, 2001; AMS, 2004). The spatial patterns of droughts are generally very complex (Vicente-Serrano, 2006) and the differences in these patterns are big in climatic transition areas as the Mediterranean basin, because

* Corresponding author at: Climatology Group, Department of Geography, University of Barcelona, Montalegre 6, 08001 Barcelona, Spain.
E-mail address: shifa.mathbout@ub.edu (S. Mathbout).

http://dx.doi.org/10.1016/j.atmosres.2017.09.016
Received 29 May 2017; Received in revised form 18 September 2017; Accepted 26 September 2017
Available online 29 September 2017
0169-8095/ © 2017 Elsevier B.V. All rights reserved.

of the complexity of the atmospheric influences.

A significant decrease in precipitation amount during the 21st century has been predicted in the Mediterranean area (Lelieveld et al., 2012; Rohde et al., 2013) and this trend is expected to continue, with a decrease of up to 20% in total annual rainfall by the year 2050 (Black, 2009; Evans, 2009; Gonçalves et al., 2014). For these reasons, the development of drought monitoring and management plans is vital for risk mitigation. Because of long periods of low precipitation (White et al., 2014; Deitch et al., 2017) and their interannual variability (Lionello, 2012), many countries in the Mediterranean region are subjected to severe and frequent droughts and their impacts (Turk et al., 2016).

Most arid and semiarid lands in the Middle East are located on marginal areas of irrigated and cultivation and are highly sensitive to periodic climate change. (Evans, 2009) and several studies have reported declining trends in terrestrial water storage over this area (Voss et al., 2013; Al Zyoud et al., 2015; Forootan et al., 2016). Many studies have highlighted the potential impacts of future climate changes on both drought frequency and severity (Sheffield and Wood, 2008; Dai, 2011; Jenkins and Warren, 2015), with some changes probably boosting severe land degradation, especially in marginal areas (Vicente-Serrano et al., 2015) where drought episodes are often responsible for most negative effects on vegetation cover and substantial losses of crop productivity (Schillinger et al., 2008; Quiroga and Suárez, 2016; Nogueira et al., 2017). General tendencies of temperature increase and precipitation decrease have been recorded over the last decades on vast areas of the Middle East (Tanarhte et al., 2012). The drought from 1998 to 2001 across this region was reported to be the worst in 50 years, affecting millions of people (ACSAD, 2011). The Middle East is conceded to be one of the driest and most water scarcity areas of the world (Evans et al., 2004; Terink et al., 2013). According to climate change projections, Syria is predicted to suffer an increased risk of severe water shortages, forest fires, loss of agricultural land and an influx of potentially invasive species (Sowers et al., 2011). Large parts of Syria experienced significant increases in the length of dry season (about 2 months longer) by late century (Evans, 2009). Rainfall represents about 70% of the available water sources in Syria (ACSAD, 2011). Moreover, the current political situations in Syria can lead to a more critical water scarcity in the nearest future. Three of the four most severe droughts on record for the country have occurred after mid-1980s (Chatel, 2014). There are a lot of evidences which consider the 2007–2010 drought as a primary indicator of the projected climatic changes in this area, including increased temperature, decreased basin rainfall and runoff, widespread crop damage, and decrease in water supply (Gleick, 2014; Skaf and Mathbout, 2010). Recent studies have referred to this period as the worst 3-year drought in the instrumental period (Trigo et al., 2010) which contributed to the present conflict in Syria. Over the last five decades, Syria experienced about 25 years of drought, which represents over 40% of the period (Breisinger et al., 2011; Al Riffaiand and Breisinger, 2012). During the season 2007–2008, the mean annual rainfall across Syria dropped by 66% of the long term average, crop failure reached 75%, and Syria experienced a humanitarian crisis accompanied with large-scale migration and widespread malnutrition (Chatel, 2014; WFP, 2014). Cook et al. (2016) have found that there is a 98% likelihood the recent drought is more severe than any comparable period during last 500 years in the Levant.

Previous climate research in the Middle East has seldom applied the SPI and *SPE*I indices to identify drought severity, and few studies focused specifically on drought in Syria (Skaf and Mathbout, 2010; Abou Zakhem and Kataa, 2016). For this reason, we are using in this study both drought indices to detect and characterize both spatial and temporal variability of drought in Syria over last five decades (i.e. 1961–2012 period). This paper is organized into 5 sections: in Section 2, we describe the objectives and study area; in Section 3, we present the database and its quality and homogeneity, and those drought indices used for drought characterisation; in section 4, we display analysis results and discussion; finally, in section 5, we derive some conclusions from the main results toward evaluating the drought risk in Syria.

2. Objectives and study area

In this study we used the Standardised Precipitation Index (SPI) and the Standardised Precipitation Evapotranspiration Index (*SPE*I) - described in detail in section 3. Our main objectives are as follows: (1) to identify regions in Syria having a common temporal variability of droughts; (2) to assess trends using both SPI and SPIE drought indices in each region at different time scales and to analyse their spatiotemporal variability.

Syria is located in south-western Asia, north of the Arabian Peninsula in the Middle East. In general, the climate of the study area is under dominant macro Mediterranean climate with a relatively cool winter and very hot summer (Bolle, 2003; Lionello et al., 2006). As corresponds to a Mediterranean climate, winter is characterized by relatively higher rainfall in comparison with the remaining seasons of the year. Spatial distribution of precipitation is highly influenced by the topographic ranges and the weather in Syria is mainly affected by the polar air masses from the Atlantic Ocean and Western Europe, which generate most of the rainfall in Syria, and the tropical air mass from North Africa, which brings dry air and leads to air-temperature above normal (Jacobeit et al., 2007; Abou Zakhem and Hafez, 2010). High rates of evaporation occur during the summer whereas the low ones in winter. The rainy season in Syria starts in September over the coastal

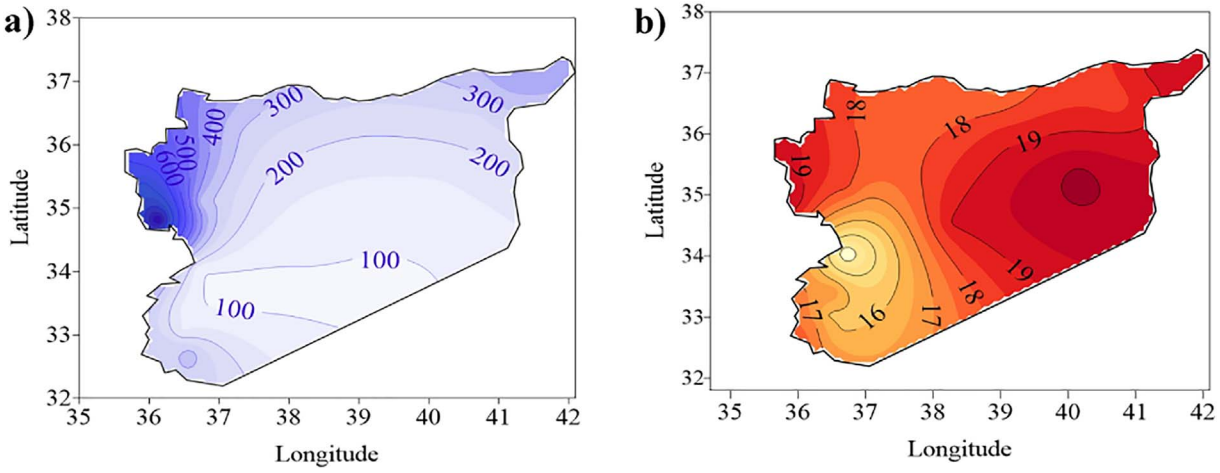

Fig. 1. Mean annual precipitation (in mm) (a) and temperature (in °C) (b) of the study area (Syria) according to the weather stations considered in this study.

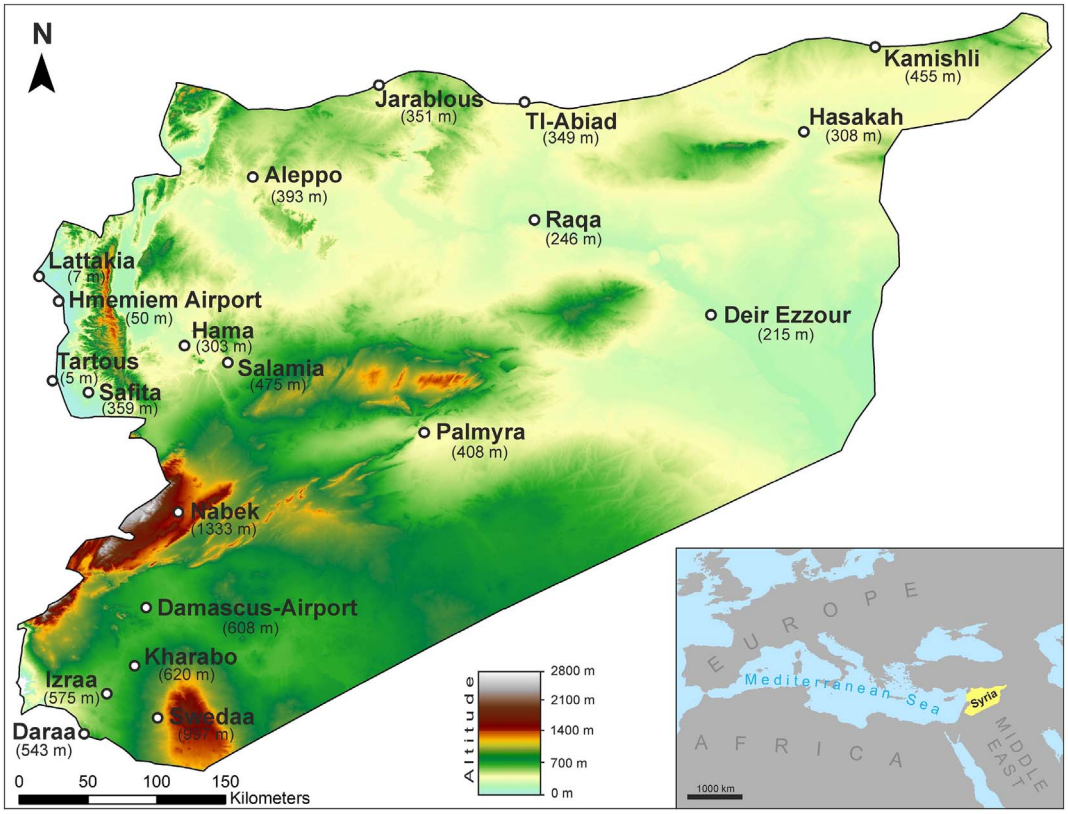

Fig. 2. Hypsometric map of Syria and spatial distribution of the meteorological stations.

and north-east areas of the country, and it spreads out by October to cover most of the country. The spatial distribution of annual precipitation over Syria is shown in Fig. 1a.

The aridity in Syria increases from west to east and north to south by decreasing of annual precipitation amounts and increasing of evapotranspiration rates. However, there are certain areas with high annual rainfall amounts (e.g. in the northwestern coastal region over the Alawiyin Mountains). The mean monthly temperature in whole country ranges from 7 °C in January to 27 °C in August. The mean annual temperature ranges from 10 and 12 °C at mountain tops of the south western parts of Syria (i.e. Lebanese eastern Mountains) to 20 °C in the eastern and south-eastern parts of the country. In the north, the mean annual temperature ranges between 15 and 19 °C (Fig. 1b). Drought forms a structural part of the semi-arid climate of Syria, with cycles of wet and dry years.

3. Data and methods

Monthly precipitation and temperature data from 20 weather stations of the Meteorological Agency of Syria were used (Fig. 2). They are mainly concentrated in the west of the country while the south-east (desert area) is far less covered. The common time period for the analysis was 1961 to 2012 (52 years). Monthly precipitation and temperature datasets were checked for homogeneity and trends. The Standard Normal Homogeneity Test (SNHT) (Alexandersson, 1986) and the Mann–Kendall trend test (MK) (Sneyers, 1990) were used for this purpose. SNHT was applied on the 52 year monthly precipitation and temperature series of 23 stations in Syria. Inhomogeneity was detected at 13% of total stations for both precipitation and temperature series. Three stations were inhomogeneous and doubtful whereas 20 stations were found to be homogeneous and useful. According to these results we discarded 3 stations (Idlib, Athria and Abu Kamal) and completed this study with 20 stations. Kriging model was applied to the spatial interpolation which is widely implemented in forestry and climatology (Lopez-Bustins et al., 2007; Appelhans et al., 2015).

3.1. The SPEI and SPI as multi-scalar drought indicators

Drought indices are important elements for drought planning and monitoring system (Zargar et al., 2011; Patel and Yadav, 2015; Bachmair et al., 2016; Wang et al., 2017). They are vital tools for supporting policy makers in mitigating drought impacts on several water sectors. Both of *SPE*I and SPI were used for Drought Early Warning in National Drought Mitigation Centre and NASA (United States), in the European Drought Centre (EDC) in Europe and in National Meteorological Agencies in the Balkan Region (Frank et al., 2017). Spatial and temporal extent and severity of droughts can be determined using drought indices (Hayes, 2000; Wang et al., 2017), which are simple or composite indicators which identify and monitor drought events (Palmer, 1965; Gibbs and Maher, 1967; Bhalme and Mooley, 1980; McKee et al., 1995; Wells et al., 2004; Vicente-Serrano et al., 2010a). To describe the temporal and spatial distribution of drought or dry spell situation, we can mainly use meteorological parameters and multivariate geostatistical approaches are commonly employed for spatial and temporal rainfall estimation (Yu et al., 2013; Mitra and Srivastava, 2017). In this study, we have used the Standardised Precipitation Index (SPI) (McKee et al., 1995) and the Standardised Precipitation Evapotranspiration Index (*SPE*I) (Vicente-Serrano et al., 2010a).

Drought indices associated with specific time-scales are useful tools for monitoring and management of drought. Several drought indices were developed by multiple authors with the objective of showing that a drought is in progress or has occurred, as well as to identify the duration, severity and spatial variability of droughts (Halwatura et al., 2015; Tsakiris, 2017). A universal meteorological drought index, Standardised Precipitation Index (SPI), recommended by the WMO and developed by McKee et al. (1993), is less complicated and used to quantify the precipitation deficit for multiple time scales, reflecting the

Table 1
The seven categories according to the Standardised Precipitation Index (SPI) and the Standardised Precipitation Evapotranspiration Index (*SPE*I) values.

SPI and *SPE*I values	Category	Cumulative Probability %
≥ 2.00	Extremely wet	2.3
1.50 to 1.99	Very wet	4.4
1.00 to 1.49	Moderately wet	9.2
− 0.99 to 0.99	Near normal	68.2
− 1.49 to − 1.00	Moderately dry	9.2
− 1.99 to − 1.50	Severely dry	4.4
≤ − 2.00	Extremely dry	2.3

impact of precipitation deficiency on the availability of various water supplies. A major assumption made in the SPI computation is that the precipitation and other meteorological variables are stationary with no temporal trends (Vicente-Serrano et al., 2010a). However, temperature plays an important role in the moisture availability and various empirical studies have shown that an increase in temperature affects the severity and duration of droughts (Rebetez et al., 2006; Griffin and Anchukaitis, 2014). Hence, a drought index based on precipitation data only may not be sufficient to monitor droughts. To accommodate dual influence of precipitation and temperature, some authors have developed new drought indices in the last decade. A multi-scalar Standardised Precipitation-Evapotranspiration Index (*SPE*I), developed by Vicente-Serrano et al. (2010a), might be very suitable for identifying drought periods, evaluating drought severity, detecting drought regional basis and measuring anomalies in climatic water balance. The *SPE*I is preferable in assessing the future water resource availability in light of recent global warming due the important effect of temperature on PET (Lopez-Bustins et al., 2013). SPI and *SPE*I were originally calculated for 3, 6, 12, 24, and 48 month time periods. These time scales reflect the different effects of drought on the availability of the various types of water resources. Usually, soil moisture conditions respond to precipitation anomalies on a relatively short scale, while ground water, streamflow, snowpeak and reservoir storage represent long-term precipitation deficit (McKee et al., 1993; Dai, 2011; Vicente-Serrano et al., 2011).

The selected drought indices SPI and *SPE*I were defined for monthly data and computed at different time scales, and identify the sub-regions characterized by different precipitation regimes and drought. Computation of SPI was carried out based on the two parameter gamma distribution function which is then transformed into a normal distribution so that the mean SPI is zero (McKee et al., 1993, 1995; Edwards and McKee, 1997). The SPI is comparable in both time and space, but it is not affected by geographical and topographical differences (Lana et al., 2001). The *SPE*I is similar to SPI but including the role of temperature and taking into account the monthly climatic water balances (P-PET). The *SPE*I is computed at multi-temporal scales based on the non-exceeding probability of precipitation and potential evapotranspiration differences (P-PET) and used for detecting and monitoring the effects of global warming on drought events (Vicente-Serrano et al., 2010a). It can detect the temporal variety of drought events more than SPI (Homdee et al., 2016). The P-PET was used to estimate the yearly changes in the degree of aridity known as aridification (Arora, 2002; Vicente-Serrano et al., 2010b; Nastos et al., 2016).

One of the most important advantages of both SPI and *SPE*I is that they can be computed at multiple time scales, which enables us to incorporate the influence of the past values of the variable in the computation (Begueria and Vicente-Serrano, 2013). In this study, variable time scales of 3, 6, 9, 12, and 24 months were selected for the estimation of both drought indices. The selected periods of time represent arbitrary time scales for precipitation deficits in relation to SPI application premises. For the SPI computation, each of the data sets is fitted to the gamma probability density function with shape parameter α and scale parameter β to define the relationship of probability to precipitation. With the equal-probability transformation the gamma cumulative distribution function converges to the standardised normal cumulative distribution function with a mean of zero and standard deviation of unity. For calculating the *SPE*I, the algorithm developed by Vicente-Serrano et al. (2010a) was used. However, the calculations are carried out using the difference between monthly precipitation (P) and potential evapotranspiration (PET) data. Monthly PET was computed following the method of Hargreaves (Hargreaves and Samani, 1985). This method calculates PET as a function of minimum and maximum air temperature and extra-terrestrial radiation. The developers of the *SPE*I recommend the use of the three parameter log-logistic distribution, based on point observation validation. SPI and *SPE*I were computed at various temporal scales using the *SPE*I package in R statistical software developed and provided by Begueria and Vicente-Serrano (2013). To better understand the behaviour of the SPI and *SPE*I indices throughout Syria, and specifically to verify if drought indices using PET instead of real ET could be adequate to foresee impacts of climate change, a trend analysis for annual and seasonal precipitation and temperature was performed for all weather stations along the study period 1961–2012. The SPI and *SPE*I R-packages have been developed to help computing these two drought indices under various data scenarios. Computation of these indices involves fitting the P and P-PET series to a suitable probability distribution. The fitted series is then transformed into standardised values that define SPI (McKee et al., 1993) and *SPE*I (Vicente-Serrano et al., 2010a) following a given classification (Vicente-Serrano et al., 2010a) (Table 1).

The frequency was calculated as the ratio between the number of occurrences in each SPI and SPEI categories and the total number of events counted for all stations in a given region and for a given SPI and *SPE*I calculated for various lags (3, 6, 9, 12, and 24 months). The aim was to identify the spatial patterns of frequency distribution of moderate, severe and extreme droughts over Syria for various SPI and *SPE*I lags based on individual station frequency distribution.

3.2. Principal component analysis

Principal Component Analysis (PCA) is a standard statistical method which is widely used as a procedure of identifying patterns in climatic and hydrological data (Smith, 2002). It is often used in climatological studies to reduce the observed variables into a smaller number of principal components that will account for most of the variance in the observed variables. This method has also been formerly applied for analysing the temporal and spatial variability of drought phenomenon (Vicente-Serrano et al., 2004, 2006; Vicente-Serrano, 2006; Santos et al., 2010; Zou et al., 2017). To identify the main spatial patterns of variability of the *SPE*I and SPI in Syria, an oblique promax PCA rotation with Kaiser Normalization for power 2 (K = 2) (Hendrickson and White, 1964) was applied in this study. This method is considered as one of the most recommended oblique rotations for recovering the underlying true “simple structure” (Richman, 1986; White et al., 1991). The Varimax orthogonal rotation was also applied, but the climate regionalization obtained was too overlapped (not shown) because of the irregular spatial distribution of weather stations throughout the study area (Fig. 2) and therefore is not reported here. For oblique rotations, e.g. promax, the factors are allowed to correlate and sums of squared loadings cannot be added to obtain a total variance. Hence, our PCA results do not show any percentage of variance.

Our PCA is carried out in a spatial mode (*S*-mode), since this mode provides areas with close temporal behaviour (Compagnucci et al., 2001; Lopez-Bustins et al., 2015). The *S*-mode PCA produces a sequence of temporal series (named Principal Components, PCs) whose (standardised) values are called PC scores. Each PC is associated with a spatial structure derived from loadings. The loadings express the observed variable as a function of the PCs and they give a spatial pattern for each PC. Those regions with absolute values of loadings > 0.4 can

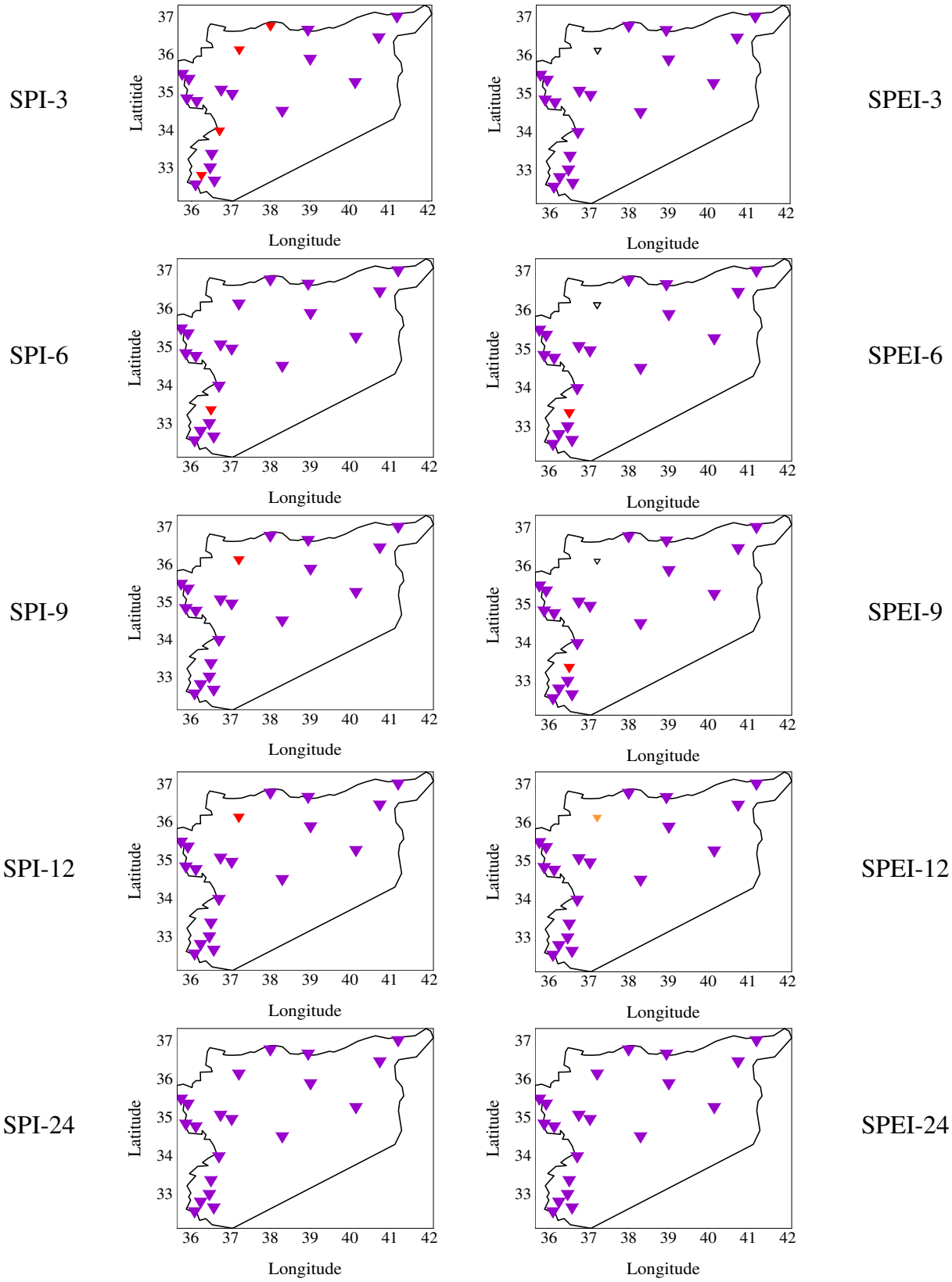

Fig. 3. Standardised Precipitation Index (SPI) and Standardised Precipitation Evapotranspiration Index (*SPEI*) trends at 3, 6, 9, 12 and 24 monthly time scale for the 20 weather stations over the 1961–2012 period. The statistical significance of the trends was checked applying the non-parametric Mann-Kendall test for the confidence levels of 95%, 99% and 99.9%
▼ Negative significant trend at 99.9%
▼ Negative significant trend at 99%
▼ Negative significant trend at 95%
▽ Non-significant negative trend.

be considered almost mutually exclusive areas (White et al., 1991). The number of PCs selected in this study was carried out according to the Scree test (Cattell, 1966). The statistical significance of PC scores trends was evaluated using the non-parametric Mann–Kendall test. The drought frequency was finally calculated following the same methodology applied to the climatic series described in 3.1.

4. Results and discussion

4.1. SPI and SPEI trends

Negative *SPE*I and SPI trends were found in all stations and the results of the Mann–Kendall test at each station for the *SPE*I at 3, 6, 9, 12, and 24 month lags are represented in Fig. 3. The amount of stations, with a negative trend at high confidence levels (99.9 and 99%), is higher when a longer time scale is considered in both indices. At 99.9% confidence level, negative trend was detected at 16 and 19 stations for SPI-3 and *SPE*I-3, respectively, at 19 and 18 stations for both indices at 6 and 9 time scales, respectively. For 12 month time scale, 19 stations detected a decreasing trend for both SPI and *SPE*I while all stations showed negative trend for SPI-24 and *SPE*I-24.

At 99% confidence level, only Kharabo station (southern Syria) showed a significant negative trend for both SPI and *SPE*I at 6 month lags and *SPE*I-9, and Aleppo station (northwestern Syria) a significant negative trend for SPI-9. Only Aleppo station showed non-significant trend for *SPE*I-3, *SPE*I-6 and *SPE*I-9. The results also indicate that no positive trend is observed at all previous stations for both *SPE*I and SPI. As the accumulation period for calculation of the *SPE*I and SPI increases (from 3 to 24 months), the persistence of drought in these regions is increasingly significant at high confidence levels (99 and 99.9%). Results, for both *SPE*I and SPI, show an intensive drought at all-time scales especially at long ones (9, 12 and 24 months) where droughts tend to aggravate considerably (Fig. 3).

All stations where a significant negative trend of the *SPE*I was detected are shown (Fig. 3). The thermic and pluviometric regimes of these stations were significantly affected by the overall big difference between precipitation and temperature (P-PET) which is a result of increasing temperature trend and decreasing precipitation trends in Eastern Mediterranean (Evans, 2009; IPCC, 2013), especially, in July–August which are the warmest and driest months (Saaroni and Ziv, 2000). Thus, in summer, the PET appeared to be more important than P in explaining drought trends, probably as a consequence of the seasonal precipitation regime characterized by low precipitation in summer months in comparison to winter and spring. Large significant positive trends in mean temperature were observed in summer in all stations, as illustrated in Fig. 4 which was built with the kriging methodology described in Lopez-Bustins et al. (2007). The positive trends in the mean temperature were due to a high significant increase in minimum temperature (not shown). This was also observed by Skaf et al. (2013) who reported a significant increase in mean temperature mainly related to the increase in minimum temperature during the warm period of the year. These results agree with Lelieveld et al. (2012) who anticipated a rapid warming in the Eastern Mediterranean and Middle East in the 21st century, especially in summer.

In summer, a significant positive trend in mean temperature was identified in 12, 4, 2 stations at 99.9, 95 and 90% confidence level, respectively, ranging from 0.05 to 0.50 °C per decade, with the highest increase in north-western Syria (Fig. 4). The largest increase in summer temperature was observed in Meslmiah (0.64 °C per decade), which is located in northwestern Syria. Considering the effect of temperature and thus the PET on drought severity enables the identification of different drought types and their impacts in the context of global warming. The 1990s constitute the warmest decade in Syria and one of the driest periods; this matter agrees with other studies in Eastern Mediterranean which proved that the 1990s and 2000s have been the warmest decades of the 20th century with 1998 the warmest year and August 1998 is the warmest month (Saaroni et al., 2003; IPCC, 2007) and the early 1990s were characterized by an extreme drought over this region (CRU, 1997).

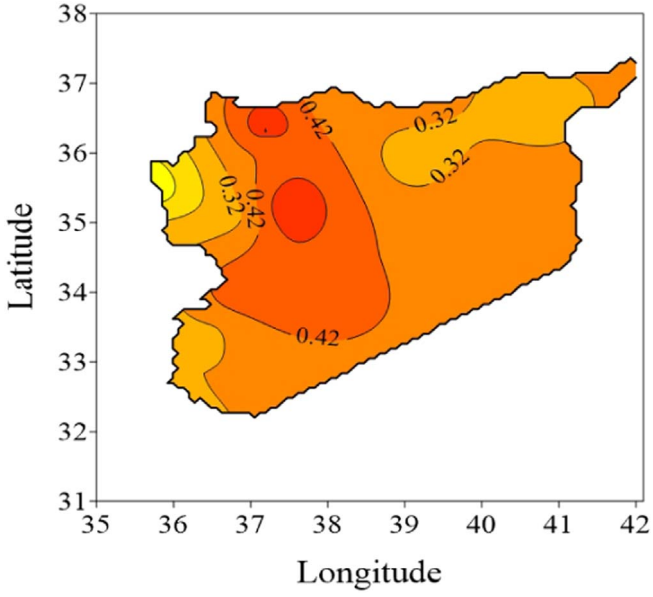

Fig. 4. Change in mean summer temperature (°C) per decade along the 1961–2012 period.

The links between climate change and drought in the Eastern Mediterranean region and in Syria were highlighted in a number of studies based on climate models, which predict that climate change will increase the risk of frequent and severe droughts, associated with warmer temperatures and lower and more unpredictable precipitation levels which will affect soil moisture and groundwater recharge (Breisinger et al., 2011). Several studies suggested that global warming may increase drought severity as a consequence of increased atmospheric evaporative demand (Dai, 2013; Vicente-Serrano et al., 2014). Our results also suggest this pattern and confirm the increase of water demand related to PET reinforced drought severity in the *SPE*I calculations relative to the SPI. PET is often modelled as a function of temperature alone, but it is influenced by solar and longwave radiation, temperature, wind speed, and humidity (McVicar et al., 2012; King et al., 2015). Thus, given the evolution of these variables, the PET could decrease as a consequence of reduced radiative forcing (Roderick and Farquhar, 2002), increased relative humidity (Jhajharia et al., 2012) and/or a decrease in wind speed (McVicar et al., 2012) which in turn can offset the influence of temperature increases on PET. At present, there are no long time series of these variables available for Syria (especially for sunshine duration or radiative forcing), and consequently no definitive conclusion can be made about if drought severity in Syria is increasing as a consequence of greater atmospheric evaporative demand. As the accumulation period for calculation of the *SPE*I and SPI increases (from 1 to 24 months), the persistence of drought in Syria is increasingly significant at high confidence levels (99 and 99.9%) which, in turn, reflects the impact of drought on the availability of different water resources. For instance, precipitation anomalies can affect soil moisture conditions on a relatively short time period whereas groundwater, stream flow, and reservoir storage reflect the long-term precipitation anomalies. For this reason, *SPE*I and SPI were originally calculated for 3, 6, 12, 24 and 48 monthly time scales (McKee et al., 1993; Vicente-Serrano et al., 2010a). The majority of stations where a significant negative trend of the *SPE*I at high confidence levels was detected are located in the western part of Syria (coastal region). The thermic and pluviometric regimes of these stations are deeply affected by the overall increasing temperature trend and decreasing precipitation trend more than other parts which usually

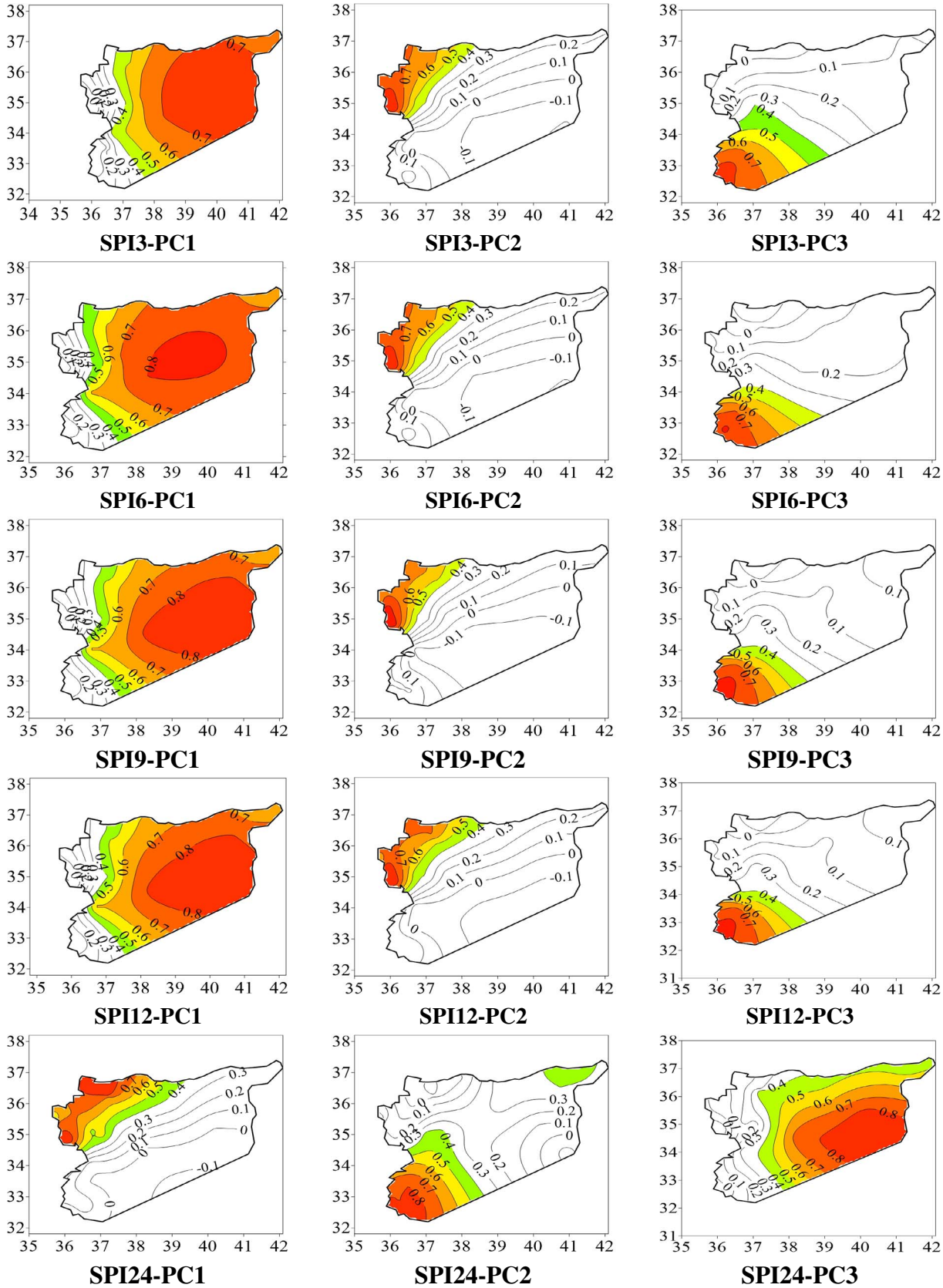

Fig. 5. Loading patterns of the three principal components (PCs) for the SPI and *SPEI* at several time scales (3, 6, 9, 12 and 24 month) for the 1961–2012 study period.

have less precipitation amounts (Abou Zakhem and Hafez, 2010). These results are coherent with the scenarios which predict a significant decrease in precipitation amount for much of western Syria by mid-century at the 95% confidence level, and by late century it might be significant at the 99% confidence level for much of the area experiencing a decrease (Evans, 2009). This decrease could be caused by

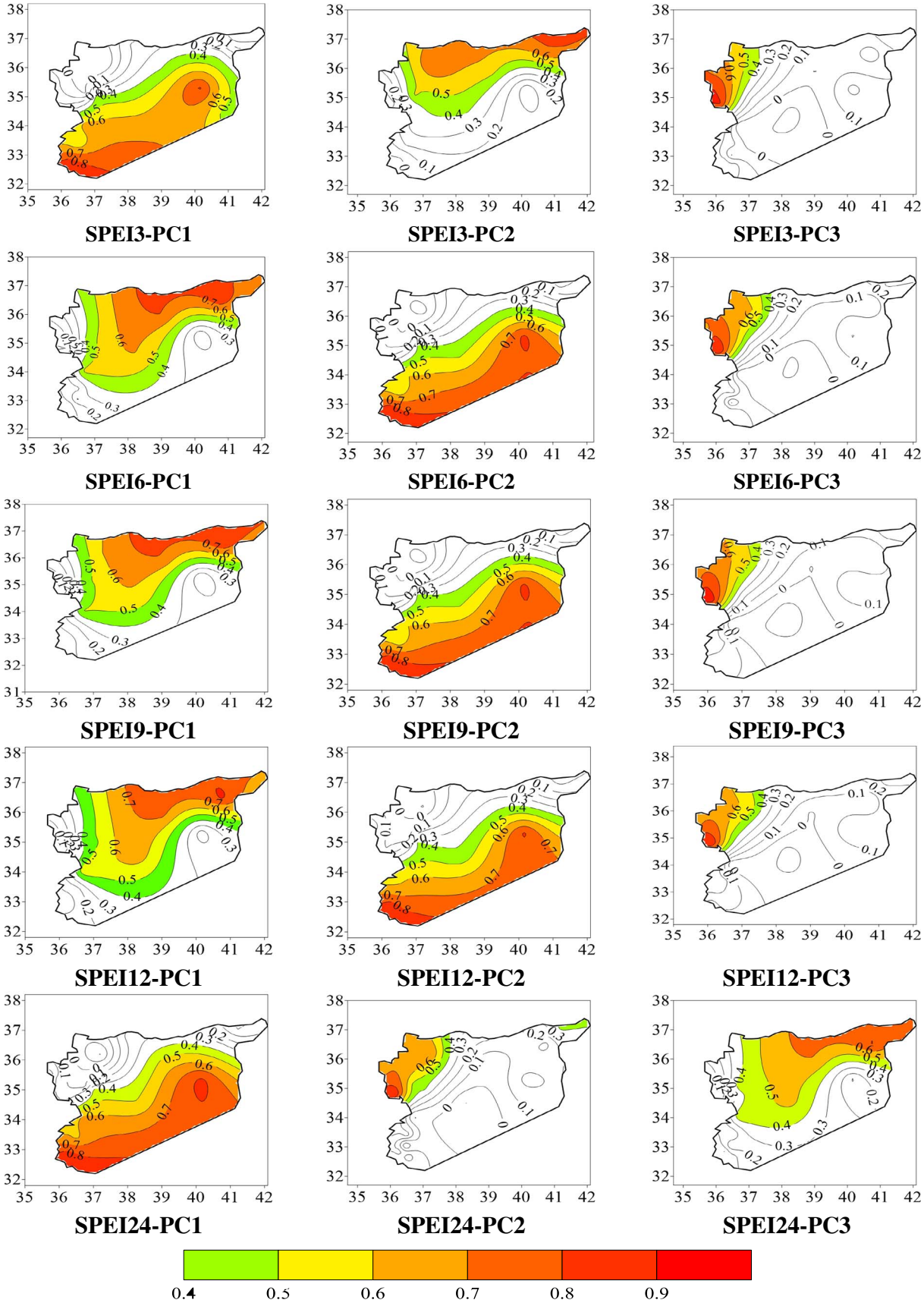

Fig. 5. (*continued*)

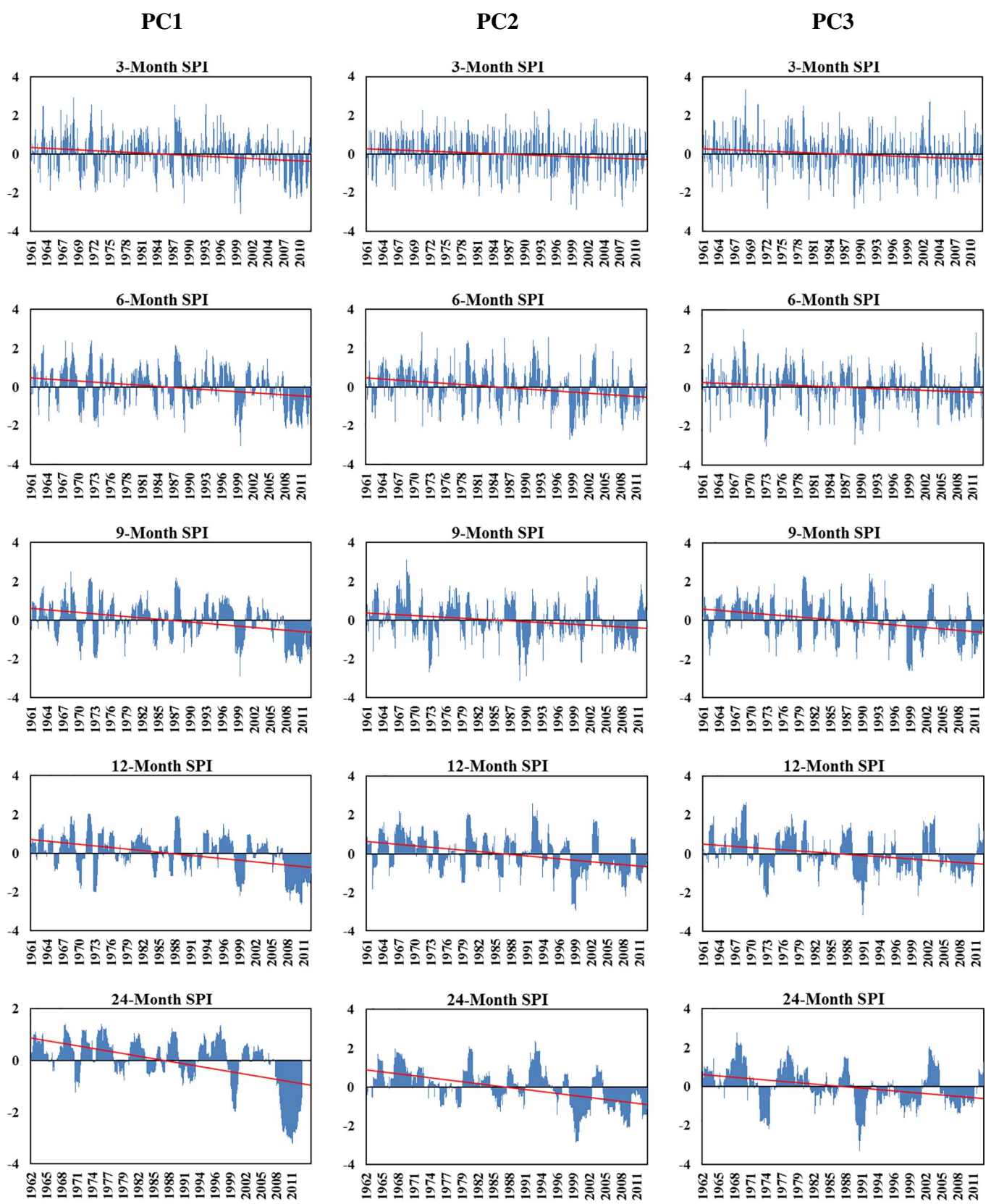

Fig. 6. Temporal evolution and trends of the 3, 6, 9, 12 and 24 month SPI and *SPEI* from the PC scores representing PC1 (northeast Syria), PC2 (south Syria) and PC3 (northwest Syria) patterns.

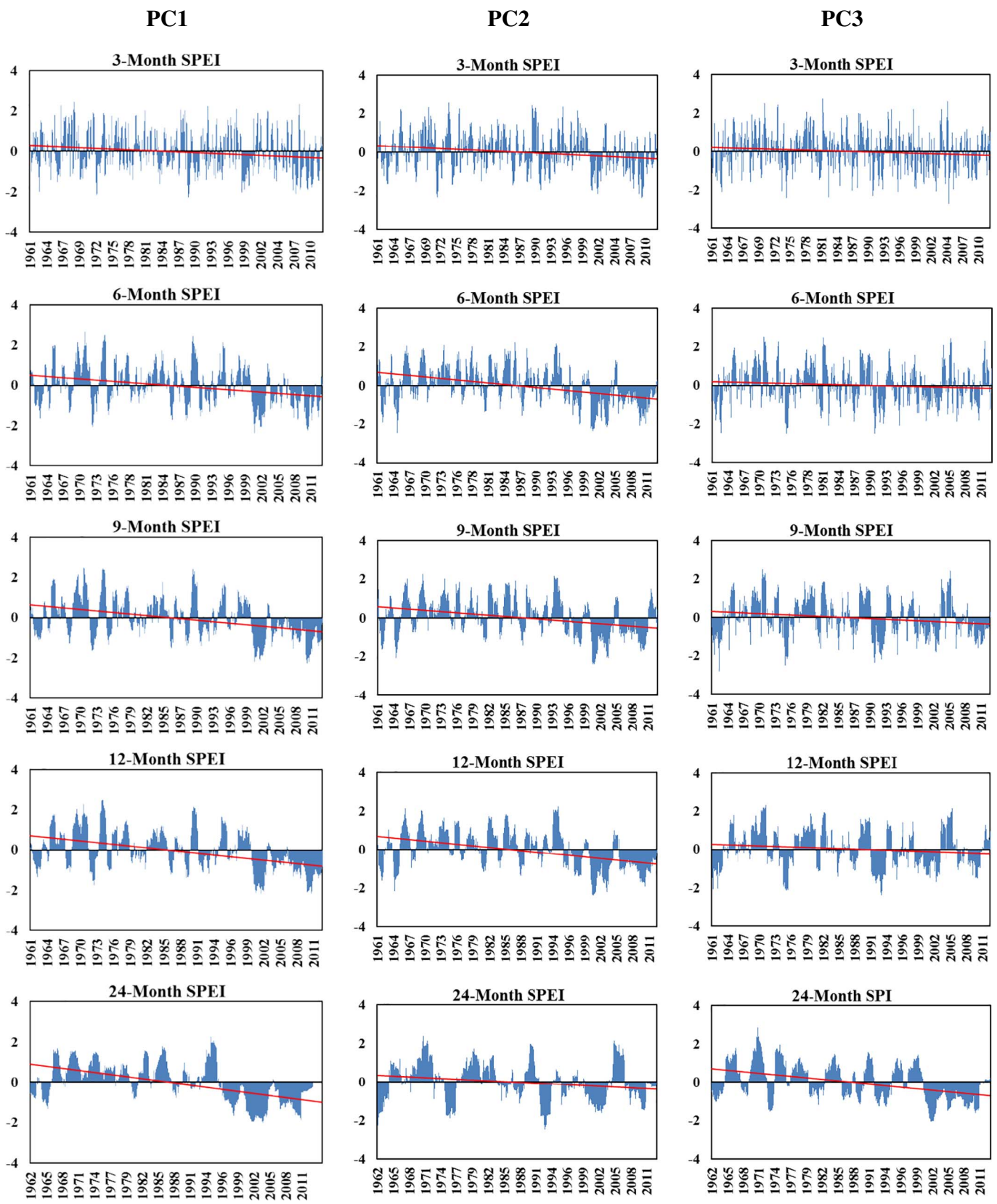

Fig. 6. (*continued*)

reduction of the storm track activity in the Eastern Mediterranean region (Evans, 2009).

4.2. Spatial and temporal variability of droughts derived from PCA

4.2.1. Loading patterns of SPEI and SPI

A subset of three components was retained in the PCA for various time sets of SPI and *SPE*I to identify sub-regions characterized by different precipitation and temperature regimes and drought variability. The loadings corresponding to each PC were mapped using the methodology described in Lopez-Bustins et al. (2007) to show the spatial patterns of drought variability across the country (Fig. 5); their associated PC scores were used for drought indices inter-comparison and trend analysis further forward. The spatial patterns of the factorial loadings obtained from PCAs using the SPI and *SPE*I series for various periods were similar at 3, 6, 9, and 12 month time scales with some differences in the order. These patterns were well structured and very coherent spatially. The differences might be explained by long dry period in Syria which exceeds three months in summer and high rates of P-PET (Fig. 5). These results indicate that the shortest time scale produces clear spatial patterns for drought evolution and show higher spatial coherence of SPI than those of *SPE*I. The results suggest that the spatial patterns of loadings identified for SPI and *SPE*I are stable throughout the 3, 6, 9, and 12 months which mean that when SPI and *SPE*I time scale change the identified subregions remain almost identical. The loadings appear to be spatially more homogeneous for SPI than *SPE*I which might reflect the effects of temperature. We considered the representative region based on absolute values of loadings larger than 0.4 (i.e., contours in the spatial map, Fig. 5) (White et al., 1991). The drought indices in different observatories were closer when the time scale was short, but for longer periods the drought conditions recorded at these observatories, in general, differed more. Based on the spatial patterns for SPI (Fig. 5) it is clear that the spatial variability of drought in Syria generally reveals the existence of three regions according to each PC: (1) PC1 north-eastern (inland desert); 2) PC2 southern (mountainous landscape); and 3) PC3 north-western (Mediterranean coast). The PC1 is characterized by the moderate precipitation in Syria with average annual precipitation about 220 mm. The PC2 is mostly high dry hills landscapes with low precipitation (the average annual precipitation is below 200 mm), while the PC3 is characterized by a high-precipitation regime with the average annual precipitation being above 700 mm (Fig. 1a). Thus, during the study period (i.e. 1961–2012) all previous regions, especially the PC1 and PC3, should reveal the precipitation deficit and positive signal of the temperature anomaly relatively more than PC2 area. This condition has been apparently caused by the global warming as a complementary cause to the precipitation deficit particularly after 1990, in certain global regions such as the Middle East (Dai et al., 2004). Depending on SPI values, no essential difference in drought evolution for these three regions was observed, but it was more clearly evident between the first two regions (i.e. PC1 and PC2) and the last one (i.e. PC3) depending on *SPE*I values resulting from the significant increase in the P-PET rates difference. The *SPE*I patterns (Fig. 5) show some differences from those obtained from SPI. The results show that the spatial patterns of loadings identified for *SPE*I are similar and the three regions appear stable when *SPE*I time scale is varied from 6 to 12 month. Change in the order has been shown for *SPE*I patterns at 3 and 24 month time scale. These differences between the *SPE*I and the SPI patterns are mainly attributed to the variation of climatic water balance across Syria dependently of the time scale of analysis and the effect of temperature variability and temperature extremes on drought conditions. Abramopoulos et al. (1988) found that the drying efficiency which resulted from temperature anomalies is as high as that due to rainfall shortage. Many authors have also confirmed that drought severity increased as a consequence temperature rise which in turn produces a higher water demand by PET (Sheffield and Wood, 2008; Dubrovsky et al., 2008; Vicente-Serrano et al., 2014).

4.2.2. Temporal analysis of SPEI and SPI scores

The temporal patterns associated with PC1, PC2 and PC3 for SPI and *SPE*I indicate some years with strong drought episodes with high and frequent fluctuation in inter-annual variability (Fig. 6). Several dry episodes were detected having large negative values, yielding critical situations for years 1960–1973, 1989, 1998, 1999, 2000, 2005, 2008, 2010 and 2012. This good temporal correlation among indicators is evident and suggest that the drought in 2008–2012 was such a long and particularly intense one in Syria, and was more intensive and detectable in the study regions depending on SPI and *SPE*I values related to the high rates of PET and less precipitation in this period especially in PC1 (north-eastern Syria) (Fig. 5). For example, the longest drought period in Syria using SPI and *SPE*I at 12 month time scale lasted 49 months and is detected in 2008–2012 which had a great impact on the area. In all regions, it seems that during the last 15–20 years, the droughts have also been longer and more intense than in the past and this is probably due to the temperature rise and precipitation decrease in Syria because of recent climate change in this area (IPCC, 2013; Evans, 2009). The results showed that a major drought from 1999 to 2001 is also detected: it was caused by a severe lack of spring and winter precipitation in three consecutive years accompanied with a severe heat wave in the year 1999 that lasted from April to September with a prolonged severe drought and extremely high temperatures for the next two years. Rainfall totals have been below normal during 1999–2001 period by 33%, 37% and 15% in PC1, PC2 and PC3, respectively and the mean temperature throughout April–September 1999–2001 period was 0.8 °C, 1.2 °C and 0.9 °C above the average in PC1, PC2 and PC3, respectively.

Many reports have suggested the 1999–2001 drought as one of the most severe drought periods during the last four decades that seriously affected crop and livestock production, and food security and safety (FAO, 2004; ESCWA, 2005). SPI detected this latter drought three months in advance than *SPE*I, but if analysed with SPI only, the drought event is not found to be as intense as *SPE*I suggest, in particular for 12 and 24 months *SPE*I. The time variability of the PC scores of all indices was examined for possible trends using a linear least square model (Fig. 6). Results show that the PC score time variability are consistent among the sub-regions, suggesting that there is an evidence for a long-term trend for drought increase in the three identified sub-regions and for both indices.

A statistically significant increasing monotonic trend in drought severity is detected for all time periods with high confidence level (99%).Very intense drought is observed for SPI-24 at the end of the study period, whereas the same drought intensity identified by *SPE*I-24 is lower but longer (since mid-1990s). These results agree with those of previous studies on the temporal analysis of droughts in Eastern Mediterranean (Lelieveld et al., 2012). For example, during years 1995–2012, maximum drought duration identified by both SPI and *SPE*I at 3 month time scale was 10–25 months, 10–28 months and 13–15 months for PC1, PC2 and PC3, respectively. The average drought duration identified by both SPI and *SPE*I for all stations in the same period was 3 to 5 months, respectively.

4.3. Drought frequency and duration

A regional frequency analysis has been performed as a method for investigating the spatial and temporal variability of droughts based on the drought intensity using the *SPE*I and SPI values of PCA scores. Drought occurrence is discussed on the basis of the frequency distribution of the SPI and *SPE*I values according to the seven classes given in Table 1. The frequency of time in each dry or wet category, expressed as the percentage of months in a given category, is shown in Fig. 7.

Both normalized indices (SPI and *SPE*I) tend to have about the same frequencies for dry and wet conditions. Results showed that the highest

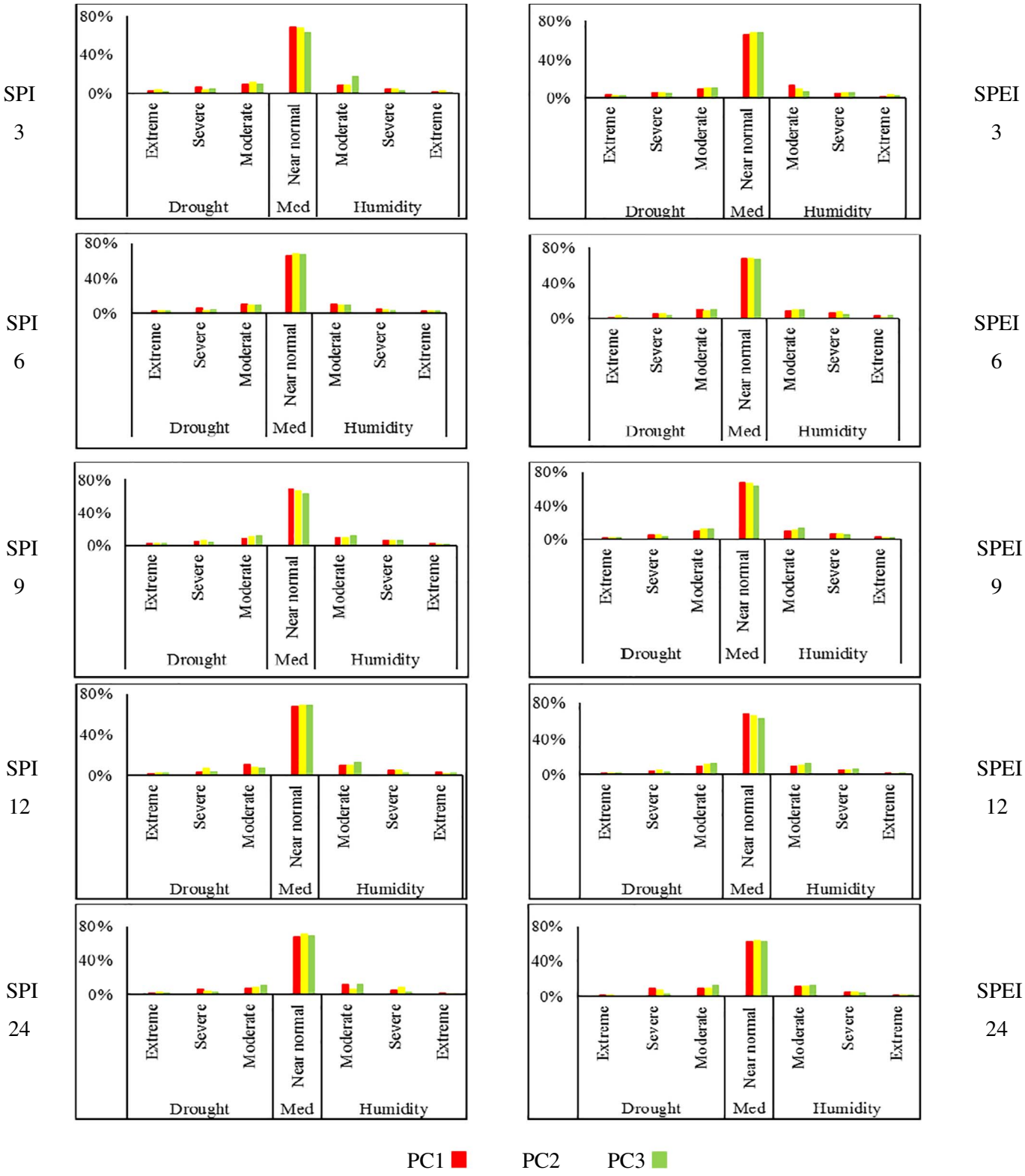

Fig. 7. Frequency of time (%) in each dry or wet category of *SPE*I and SPI in the three climate Syrian regions (PC1: northeast; PC2: south; PC3: northwest) along 1961–2012.

percentage of drought occurrence was detected by *SPE*I rather than by SPI especially at long time scales (12 and 24 month) in all regions, and the highest frequency was reported in northeast Syria (PC1), which is characterized by low precipitation and high PET. For example, greater number of extreme, severe and moderate droughts for the 12 month time scale is identified with the *SPE*I rather than with the SPI in PC1 (northeast Syria) (15.0% vs17.7%).

The highest frequency of extreme drought, which ranged between 2.4% and 3.2%, was identified in PC2 for SPI-3, SPI-6, SPI-12 and SPI-24, and in PC3 for SPI-9. On the other hand, for the *SPE*I index, the highest percentage of extreme drought occurrence was detected in both PC2 and PC3 at 12 and 24 month lags, respectively. At the shorter time scales, the highest frequencies of extreme drought showed in PC2 and PC1 at 6 and 3 month time scales, respectively. The highest numbers for

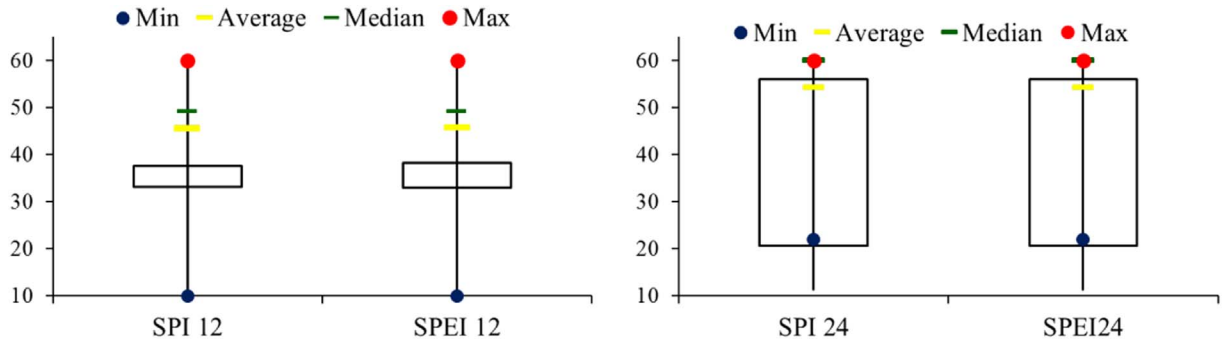

Fig. 8. Duration of drought for SPI and *SPE*I surmises on 2008–2012 period (60 months) at 12 (left) and 24 time scales (right).

the severe drought occurred in PC1 for SPI-3, SPI-6, SPI-9 and SPI-24, and in PC2 for SPI-12. For *SPE*I and overall Syria, the highest values of severe drought frequency were detected in PC2 at 3, 9 and 12 month time scales ranging 5.1–5.3% and in PC1 for 6 and 24 month time scales with a high frequency at *SPE*I-24 (9.6%) in PC2.

The results showed that the normal conditions represent 65–69% and 62–67% of the total values of SPI and *SPE*I, respectively. Those moderate conditions (wet and dry) are almost concentrated in PC3, which have the highest rates of precipitation and lowest rates of evapotranspiration. The extreme wet conditions are almost equally distributed around 10% in all regions being more frequent in the PC3. The SPI and *SPE*I show an increase in drought frequency in the period studied and an increasing tendency toward more intensive and prolonged dry episodes.

The drought duration is defined as the period of rainfall deficit (the time period between the start of the drought and its end). This is assumed as being the number of consecutive months (time intervals) with negative SPI or *SPE*I values, and the cumulative sum of indices values during the drought event known as the drought magnitude (Dracup et al., 1980, McKee et al., 1993). To facilitate the evaluation of drought duration for both SPI and *SPE*I during 2008–2012 period and to allow a comparison between both indices at 12 and 24 month time scales, the statistical characters were conducted for each timescale using a box plot. Both drought duration and magnitude for the period 2008–2012 were computed (Fig. 8). The results demonstrate that the most severe dry period was detected between 2008 and 2012 (Fig. 6) and both SPI and *SPE*I at 12 and 24 month lags showed the highest drought severity with no evident difference between their values. The average SPI and *SPE*I values are −1.11 vs −1.01 at 12 month time scale, −1.47 vs −1.20 at 24 month time scale, respectively.

The average duration for SPI-12 and *SPE*I-12 is similar (45.6 months) whereas the average duration for the SPI-24 and *SPE*I-24 ranged between 54.1 and 54.3 months. Seven stations have consecutive dry months for SPI-12 and *SPE*I-12 (for the whole study period 1961–2012) with a magnitude ranging from −5.9 to −3.2, and from −13.8 to −5.1, respectively. Drought durations were much longer for SPI-24 (55.8 months) and *SPE*I-24 (56.1 months) for the 2008–2012 period. 14 stations out of 20 showed a dry consecutive duration for the whole study period (60 months) with high severity values. During the 1961–2012 period, the magnitude ranges from-1.7 to −5.9 for SPI-12 and from −2.3 to −6.8 for SPI-24, from −2.4 to −13.8 for *SPE*I-12 and from −2.1 to −20.8 for *SPE*I-24. The big differences in SPI and *SPE*I magnitude were most detectable in dry regions which reflect the evident role of temperature and thus the evapotranspiration especially in severe drought episodes. However, few statistical studies have aimed to compare different drought indices which may allow recommending the preferential use of one of them based on objective criteria (Keyantash and Dracup, 2002; Quiring, 2009; Vicente-Serrano et al., 2010c; Anderson et al., 2011).

FAO and World Food Program (WFP) reported that up to 60% of lands in Syria experienced one of the worst long-term droughts in modern history during this period (2008–2012) and the recent conflict will exacerbate the dangers throughout whole ecologic and socio-economic systems in absence of drought risk management investments and programs. The humanitarian crisis which followed the severe drought period 2005–2010 can be seen as the result of 50 years of mismanagement of natural resources, and the Syrian government's water and agricultural policies failure as reported by Chatel (2014). It is therefore important to consider this drought period as a possible cause in the 2011 uprising during 50 years of natural resource mismanagement, rapid economic liberalization, sudden cancellation of state support and the government's failure to tackle the human and environmental crisis which can be extended for more than a decade.

5. Conclusions

The spatio-temporal evolution of droughts during 1961–2012 was investigated using the SPI and *SPE*I indices in Syria an approach seldom used in previous studies for that country. Applying an oblique promax rotation in PCA to both drought indices *SPE*I and SPI at different time scales we identified three sub-regions with different temporal behaviour of drought representing the northeast (PC1), south (PC2) and northwest (PC3) regions of Syria. Results of both drought indices are similar in the identification of the subregions and regarding the scores. The results demonstrated the *SPE*I advantage over SPI due to its capability in identifying and exploring the role of evapotranspiration and temperature variability in drought characteristics and thus the ability of *SPE*I in detecting drier conditions than the SPI. Studying of temporal evolution of averaged SPI and *SPE*I during the last five decades showed an increasing in their frequency, severity and duration. These results showed that the longest and most intense dry period was 2008–2012 followed by the periods 1999–2001, 1972–1974 and 1983–1985. On a regional scale, there is a clear evidence of a statistically significant increase in the severity and intensity of drought along the last decade (1999–2012). The main results showed that the majority of extreme drought periods were recorded within the wet period (October to May) in all three regions and the majority of longest dry periods were recorded in PC1 (north-eastern Syria) and PC2 (southern Syria) regions. The most recent and severe 2008–2012 drought had motivational impacts, contributing according to previous studies to agricultural failure, rapid economic decline, growing poverty, population displacement and political unrest in the country. Finally, results presented suggest that the methodology employed in this study can be used to monitor effectively drought conditions in Syria. This is relevant as there is an urgent need to envisage an efficient development of sustained Drought Early Warning System, preparation of drought management plans for drought mitigation and long term strategies for water management for economic, social development, and environmental sustainability.

Acknowledgments

This study was performed within the framework of Climatology

Group of the University of Barcelona (2014 SGR 300, Catalonia Regional Govt) and the WEMOTOR (CSO2014-55799-C2-1-R 2015-2017, Spanish Ministry of Economy and Competitiveness) project. The first author is supported by a grant of ERASMUS MUNDUS (AVEMPACE mobility Scheme III). All meteorological data was obtained from the Meteorological Agency in Syria (http://www.meteo.sy/). We wish to thank Dr. Rui Filipe Ferreira Carvalho in the Department of Geography, University of Barcelona, for his help.

Appendix A. Supplementary data

Supplementary data associated with this article can be found in the online version, at doi: https://doi.org/10.1016/j.atmosres.2017.09.016. These data include the Google map of the most important areas described in this article.

References

Abou Zakhem, A., Hafez, R., 2010. Climatic factors controlling chemical and isotopic characteristics of precipitation in Syria. Hydrol. Process. 24 (18), 2641–2654.

Abou Zakhem, B., Kataa, B., 2016. Cumulative drought effect on Figeh karstic spring discharge (Damascus basin, Syria). J. Environ. Earth Sci. 75, 125. http://dx.doi.org/10.1007/s12665-015-5013-3.

Abramopoulos, F., Rosenzweig, C., Choudhury, B., 1988. Improved ground hydrology calculations for global climate models (GCMs): Soil water movement and evapotranspiration. J. Clim. 1, 921–941.

ACSAD, 2011. Drought vulnerability in the Arab region: case study; drought in Syria—ten years of scarce water (2000 – 2010). In: ISDR and the Arab Centre for the Studies of Arid Zones and Dry Lands, (74 pp.).

Al Riffai, P., Breisinger, C., 2012. Droughts in Syria: an assessment of impacts and options for improving the resilience of the poor. Q. J. Int. Agric. 51 (1), 21–49.

Al Zyoud, S., Rühaak, W., Forootan, E., Sass, I., 2015. Over exploitation of groundwater in the centre of Amman Zarqa basin-Jordan: evaluation of well data and GRACE satellite observations. Resources 4, 819–830. http://dx.doi.org/10.3390/resources4040819.

Alexandersson, H., 1986. A homogeneity test applied to precipitation data. Int. J. Climtol. 6, 661–675.

AMS, (American Meteorological Society), 2004. Statement on meteorological drought. Bull. Am. Meteorol. Soc. 85, 771–773.

Anderson, M.C., Hain, C., Wardlow, B., Pimstein, A., Mecikalski, J.R., Kustas, W.P., 2011. Evaluation of drought indices based on thermal remote sensing of evapotranspiration over the continental United States. J. Clim. 24, 2025–2044.

Appelhans, T., Mwangomo, E., Hardy, D.R., Hemp, A., Nauss, T., 2015. Evaluating machine learning approaches for the interpolation of monthly air temperature at Mt. Kilimanjaro, Tanzania. Spat. Stat. 14, 91–113.

Arora, V.K., 2002. The use of the aridity index to assess climate change effect on annual runoff. J. Hydrol. 265, 164–177.

Awchi, T., Kalyana, M., 2017. Meteorological drought analysis in northern Iraq using SPI and GIS. Water Resour. Manag. http://dx.doi.org/10.1007/s40899-017-0111-x.

Bachmair, S., Stahl, K., Collins, K., Hannaford, J., Acreman, M., Svoboda, M., Knutson, C., Smith, K.H., Wall, N., Fuchs, B., Crossman, N.D., Overton, I.C., 2016. Drought indicators revisited: the need for a wider consideration of environment and society. Wiley Interdiscip. J.Clim.

Begueria, S., Vicente-Serrano, S.M., 2013. Package 'SPEI' v 1.6: calculation of the Standardised Precipitation-Evapotranspiration Index. http://cran.r-project.org/web/packages/SPEI/SPEI.pdf.

Bhalme, H.N., Mooley, D.A., 1980. Large-scale drought/floods and monsoon circulation. Mon. Weather Rev. 108 (8), 1197–1211.

Black, E., 2009. The impact of climate change on daily precipitation statistics in Jordan and Israel. Atmos. Sci. Lett. 10, 192–200.

Bolle, H.-J., 2003. Climate, climate variability, and impacts in the Mediterranean area: an overview. In: Bolle, H.-J. (Ed.), Mediterranean climate—variability and trends. Springer, Berlin, pp. 5–86.

Breisinger, C., Zhu, T., AL-Riffai, P., Nelson, G., Robertson, R., Funes, J., Verner, D., 2011. Global and local economic impacts of climate change in Syria and options for adaptation. In: Development strategy and governance division. Discussion Paper 01091 (International Food Policy Research Institute). Climate Change in Syria and Options for Adaptation.

Cattell, R.B., 1966. The scree test for the number of factors. Multivar. Behav. Res. 1, 245–276.

Chatel, F., 2014. The role of drought and climate change in the Syrian uprising: untangling the triggers of the revolution. Middle East. Stud. 50 (4), 521–535.

Compagnucci, R.H., Salles, M.A., Canziani, P.O., 2001. The spatial and temporal behaviour of the lower stratospheric temperature over the Southern Hemisphere: the MSU view. Part I: data, methodology and temporal behaviour. Int. J. Climatol. 21, 419–437.

Cook, B.I., Anchukaitis, K.J., Touchan, R., Meko, D.M., Cook, E.R., 2016. Spatiotemporal drought variability in the Mediterranean over the last 900 years. J. Geophys. Res. http://dx.doi.org/10.1002/2015JD023929.

CRU, 1997. Annual 1995. Climate Monitor. 24 (5) Climate Research Unit, Norwich.

Dai, A., 2011. Characteristics and trends in various forms of the Palmer Drought Severity Index during 1900–2008. J. Geophys. Res. 116, D12115. http://dx.doi.org/10.1029/2010JD015541.

Dai, A., 2013. Increasing drought under global warming in observations and models. Nat. Clim. Chang. 3, 52–58.

Dai, A., Trenberth, E.K., Qian, T.T., 2004. A global data-set of Palmer Drought Severity Index for 1870-2002: relationship with soil moisture and effects of surface warming. J. Hydrometeorol. 5 (6), 1117–1130.

Deitch, M.J., Sapundjieff, M.J., Feirer, S.T., 2017. Characterizing precipitation variability and trends in the world's Mediterranean-Climate areas. Water 7 (9), 259. http://dx.doi.org/10.3390/w9040259.

Deo, R.C., Sahin, M., 2015. Application of the artificial neural network model for prediction of monthly standardized precipitation and evapotranspiration index using hydrometeorological parameters and climate indices in eastern Australia. Atmos. Res. 161 (162), 65–81.

Deo, R.C., Kisi, O., Singh, V.P., 2017. Drought forecasting in eastern Australia using multivariate adaptive regression spline, least square support vector machine and M5Tree model. Atmos. Res. 184, 149–175.

Dracup, J.A., Lee, K.S., Paulson, E.D., 1980. On the definition of droughts. Water Resour. Res. 16, 297–302.

Dubrovsky, M., Svoboda, M.D., Trnka, M., Hayes, M.J., Wilhite, D.A., Zalud, Z., Hlavinka, P., 2008. Application of relative drought indices in assessing climate-change impacts on drought conditions in Czechia. Theor. Appl. Climatol. 96, 155–171.

Edwards, D.C., McKee, T.B., 1997. Characteristics of 20th century drought in the United States at multiple time scales. Atmos. Sci. Pap. 634, 1–30.

ESCWA, (Economic and Social Commission for Western Asia), 2005. ESCWA Water Development Report 1: Vulnerability of the Region to Socio-Economic Drought. United Nations, New York.

Evans, J.P., 2009. 21st century climate change in the Middle East. J. Clim. Chang. 92, 417–432.

Evans, J.P., Smith, R.B., Oglesby, R.J., 2004. Middle East climate simulation and dominant precipitation processes. Int. J. Climatol. 24, 1671–1694.

FAO, (Food and Agriculture Organization), 2004. Syrian Arab Republic: capacity building in drought early warning system for the Syrian rangelands. In: Syrian project document, TCP/SYR/3002 (T), May.

Forootan, E., Safari, A., Mostafaie, A., Schumacher, M., Delevar, M., Awange, J.I., 2016. Large-scale total water storage and water flux changes over the arid and semi-arid parts of the Middle East from GRACE and reanalysis products. Surv. Geophys. http://dx.doi.org/10.1007/s10712-016-9403-1.

Frank, A., Amenski, T., Gocicc, M., Popov, S., Popovice, L., Tajkovic, S., 2017. Influence of mathematical and physical background of drought indices on their complementarity and drought recognition ability. Atmos. Res. 194, 268–280.

Gibbs, W.J., Maher, J.V., 1967. Rainfall Deciles as Drought Indicators. Bureau of Meteorology Bulletin No. 48 Commonwealth of Australia, Melbourne, pp. 29.

Gleick, P.H., 2014. Water, drought, climate change, and conflict in Syria. Bull. Am. Meteorol. Soc. 6, 331–340.

Gonçalves, M., Barrera Escoda, A., Guerreiro, D., Baldasano, J.M., Cunillera, J., 2014. Seasonal to yearly assessment of temperature and precipitation trends in the North Western Mediterranean Basin by dynamical downscaling of climate scenarios at high resolution (1971–2050). Clim. Chang. 122 (1), 243–256.

Griffin, D., Anchukaitis, K.J., 2014. How unusual is the 2012–2014 California drought? Geophys. Res. Lett. 41, 9017–9023.

Halwatura, D., Lechner, A.M., Arnold, S., 2015. Drought severity–duration–frequency curves: a foundation for risk assessment and planning tool for ecosystem establishment in post-mining landscapes. Hydrol. Earth Syst. Sci. 19, 1069–1091.

Hargreaves, G.H., Samani, Z.A., 1985. Reference crop evapotranspiration from temperature. Trans. ASAE 1 (2), 96–99.

Hayes, M.J., 2000. Revisiting the SPI: clarifying the process. Drought Network News 1, 13–14.

Heim, R.R., 2002. A review of twentieth-century drought indices used in the United States. Bull. Am. Meteorol. Soc. 83, 1149–1165.

Hendrickson, A.E., White, P.O., 1964. Promax: a quick method for rotation to oblique simple structure. Br. J. Math Stat. Psychol. 17, 65–70.

Homdee, T., Pongput, K., Kanae, S., 2016. A comparative performance analysis of three standardized climatic drought indices in the Chi River basin, Thailand. Agric. Nat. Resour. 50, 211–219.

IPCC, 2013. Summary for policymakers, in climate change. In: Stocker, T.F., Qin, D., Plattner, G.K., M Tignor, M., Allen, S.K., Boschung, J., Nauels, A., Xia, Y., Bex, V., Midgley, P.M. (Eds.), The Physical Science Basis. Contribution of Working Group I to the Fifth Assessment Report of the Intergovernmental Panel on Climate Change. Cambridge University Press, Cambridge, United Kingdom and New York, NY, USA.

IPCC (Intergovernmental Panel on Climate Change), 2007. Climate change 2007—the physical science basis. In: Contribution of Working Group I to the Fourth Assessment Rep. of the Intergovernmental Panel on Climate Change. Cambridge University Press, Cambridge, U.K..

Jacobeit, Dünkeloh, A., Hertig, E, 2007. Mediterranean rainfall changes and their causes. In: Lozán, Graß, H., Hupfer, P., Menzel, L., Schönwiese, C.D. (Eds.), Global Change: Enough Water for all? Wissenschaftliche Auswertungen, Hamburg, Germany, pp. 195–199.

Jenkins, K., Warren, R., 2015. Quantifying the impact of climate change on drought regimes using the standardised precipitation index. Theor. Appl. Climatol. 120, 41–54.

Jhajharia, D., Dinpashoh, Y., Kahya, E., Singh, V.P., Fakheri-Fard, A., 2012. Trends in reference evapotranspiration in the humid region of northeast India. Hydrol. Process. 26, 421–435.

Kastopoulou, E., Giannakopoulos, C., Krapsiti, D., Karali, A., 2017. Temporal and Spatial Trends of the Standardized Precipitation Index (SPI) in Greece Using Observations and Output from Regional Climate Models. In: Perspectives on Atmospheric Sciences.

Springer Atmospheric Science, pp. 75–481.
Keyantash, J., Dracup, J.A., 2002. The quantification of drought: an analysis of drought indices. Bull. Am. Meteorol. Soc. 83 (8), 1167–1180.
King, D.A., Bachelet, D.M., Symstad, A.J., Ferschweiler, K., Hobbins, M., 2015. Estimation of potential evapotranspiration from extraterrestrial radiation, air temperature and humidity to assess future climate change effects on the vegetation of the Northern Great Plains, USA. Ecol. Model. 297, 86–97.
Lana, X., Serra, C., Burgueño, A., 2001. Patterns of monthly rainfall shortage and excess in terms of the standardized precipitation index. Int. J. Climatol. 21, 1669–1691.
Lelieveld, J., Hadjinicolaou, P., Kostopoulou, E., Chenoweth, J., El Maayar, M., Giannakopoulos, C., Hannides, C., Lange, M., Tanarhte, M., Tyrlis, E., Xoplaki, E., 2012. Climate change and impacts in the Eastern Mediterranean and the Middle East. Clim. Chang. 114, 667–687. http://dx.doi.org/10.1007/s10584-012-0418-4.
Lionello, P. (Ed.), 2012. The Climate of the Mediterranean Region: From the Past to the Future. Elsevier (502 pp.).
Lionello, P., Malanotte-Rizzoli, P., Boscolo, R. (Eds.), 2006. Mediterranean climate variability. Elsevier, Amsterdam.
Lo Conti, F., Hsu, K.-L., Noto, L.V., Sorooshian, S., 2014. Evaluation and comparison of satellite precipitation estimates with reference to a local area in the Mediterranean Sea. Atmos. Res. 138, 189–204. https://doi.org/10.1016/j.atmosres.2013.11.011.
Lopez-Bustins, J.A., Esteban, P., Labitzke, K., Langematz, U., 2007. The role of the stratosphere in Iberian Peninsula rainfall: a preliminary approach in February. J. Atmos. Terr. Phys 69, 1471–1484.
Lopez-Bustins, J.A., Pascual, D., Pla, E., Retana, J., 2013. Future variability of droughts in three Mediterranean catchments. Nat. Hazards 69, 1405–1421.
Lopez-Bustins, J.A., Serrano, E., Ayarzagüena, B., Sanchez-Lorenzo, A., 2015. Spatial and temporal temperature trends in the lower stratosphere during the extended boreal winter from reanalyses. Int. J. Climatol. 35, 3888–3901.
Martín Vide, J., Olcina, C.J., 2001. Climas y tiempos de España. Alianza, Madrid (264 pp.).
McCabe, G.J., Wolock, D.M., 2015. Variability and trends in global drought. Int. J. Earth Sci. 223–228. http://dx.doi.org/10.1002/2015EA000100.
McKee, T.B., Doesken, N.J., Kleist, J., 1993. The relationship of drought frequency and duration to time scales. In: Proceeding of the 8th Conference on Applied Climatology. American Meteorological Society, Boston, pp. 179–184.
McKee, T.B., Doesken, N.J., Kleist, J., 1995. Drought monitoring with Multiple Time scales. In: In Proceeding of the Ninth Conference on Applied Climatology. American Meteorological Society, Dallas, TX, pp. 233–236.
McVicar, T.R., Roderick, M.L., Donohue, R.J., Li, L.T., Van Niel, T.G., Thomas, A., Grieser, J., Jhajharia, D., Himri, Y., Mahowald, N.M., Mescherskaya, A.V., Kruger, A.C., Rehman, S., Dinpashoh, Y., 2012. Global review and synthesis of trends in observed terrestrial 681 near-surface wind speeds: implications for evaporation. J. Hydrol. 416–417, 182–205.
Mitra, S.S., Srivastava, P., 2017. Spatiotemporal variability of meteorological droughts in southeastern USA. Nat. Hazards 86 (3), 1007–1038.
Mohammed, R., Scholz, M., 2017. Impact of evapotranspiration formulations at various elevations on the reconnaissance drought index. Water Resour. Manag. 31 (1), 531–548.
Nastos, P.T., Politi, N., Kapsomenakis, J., 2016. Spatial and temporal variability of the Aridity Index in Greece. Atmos. Res. 119, 140–152.
Nogueira, C., Bugalho, M.N., Pereira, J.S., Caldeira, M.C., 2017. Extended autumn drought, but not nitrogen deposition, affects the diversity and productivity of a Mediterranean grassland. Environ. Exp. Bot. 138, 99–108.
Palmer, W.C., 1965. Meteorological Drought, Research Paper No. 45. U.S. Department of Commerce Weather Bureau, Washington, DC.
Patel, N.R., Yadav, K., 2015. Monitoring spatio-temporal pattern of drought stress using integrated drought index over Bundelkhand region, India. Nat. Hazards 77 (2), 663–677.
Quiring, S.M., 2009. Developing objective operational definitions for monitoring drought. J. Appl. Meteorol. Climatol. 48, 1217–1229.
Quiroga, S., Suárez, S., 2016. Climate change and drought effects on rural income distribution in the Mediterranean: a case study for Spain. Nat. Hazards Earth Syst. Sci. 16, 1369–1385.
Rebetez, M., Mayer, H., Dupont, O., Schindler, D., Gartner, K., Kropp, J., Menzel, A., 2006. Heat and drought 2003 in Europe: a climate synthesis. Ann. For. Sci. 63, 569–577.
Retalis, A., Katsanos, D., Michaelides, S., 2016. Precipitation climatology over the Mediterranean Basin—Validation over Cyprus. Atmos. Res. 169, 449–458.
Richman, M.B., 1986. Rotation of principal components. Int. J. Climatol. 6, 293–335. http://dx.doi.org/10.1002/joc.3370060305.
Roderick, M.L., Farquhar, G.D., 2002. The cause of decreased pan evaporation over the past 50 years. Science 298, 1410–1411.
Rohde, R., Muller, R.A., Jacobsen, R., Muller, E., Perlmutter, S., Rosenfeld, A., Wurtele, J., Groom, D., Wickam, C., 2013. A new estimate of the average earth surface land temperature spanning 1753 to 2011. Geoinfor Geostat.: An Overview 1, 1–7.
Saaroni, H., Ziv, B., 2000. Summer rainfall in a Mediterranean Climate - the case of Israel: climatological - dynamical analysis. Int. J. Climatol. 20, 191–209.
Saaroni, H., Ziv, B., Edelson, J., Alpert, P., 2003. Long-term variations in summer temperatures over the Eastern Mediterranean. Geophys. Res. Lett. 30 (18), 1946. http://dx.doi.org/10.1029/2003GL017742.
Santos, J.F., Pulido-Calvo, I., Portela, M.M., 2010. Spatial and temporal variability of droughts in Portugal. Water Resour. Res. 46, W03503. http://dx.doi.org/10.1029/2009WR008071.
Schillinger, W.F., Schofstoll, S.E., Alldredge, J.R., 2008. Available water and wheat grain yield relations in a Mediterranean climate. Field Crop Res. 109 (1–3), 45–49.
Sheffield, J., Wood, E.F., 2008. Projected changes in drought occurrence under future global warming from multi-model, multi-scenario, IPCC AR4 simulations. Clim. Dyn. 31, 79–105.
Skaf, M., Mathbout, S., 2010. Assessment of drought severity and frequency in Arid Syrian regions by SPI index. AJ Arid. Environ. 3, 98–103.
Skaf, M., Abou Zakhem, A., Mathbout, S., 2013. Temperature Changes in Semi-Arid, Arid and Extreme Arid Regions of Syria and Their Potential Effects on Vegetation. The J. A J. Arid Environ. 6 (2), 42–54.
Smith, L.I. (Ed.), 2002. A Tutorial on Principal Components Analysis. Computer Sciences 26, University of Otago, Dunedin, New Zealand.
Sneyers, R., 1990. On statistical analysis of series of observations. WMO Technical note No. 143, WMO No. 415 (Geneva, Switzerland, 192 pp.).
Sowers, J., Vengosh, A., Weinthal, E., 2011. Climate change, water resources, and the politics of adaption in the Middle East and Nortfh Africa. Clim. Chang. 104, 599–627.
Surendran, U., Kumar, V., Ramasubramoniam, Raja, P., 2017. Development of Drought Indices for Semi-Arid Region Using Drought Indices Calculator (DrinC) - a case study from Madurai District, a semi-arid region in India. Water Resour. Manag. http://dx.doi.org/10.1007/s11269-017-1687-5.
Tanarhte, M., Hadjinicolaou, P., Lelieveld, J., 2012. Intercomparison of temperature and precipitation data sets based on observations in the Mediterranean and the Middle East. J. Geophys. Res. Atmos. 117, D12102. http://dx.doi.org/10.1029/2011JD017293.
Terink, W., Immerzeel, W.W., Droogers, P., 2013. Climate change projections of precipitation and reference evapotranspiration for the Middle East and Northern Africa until 2050. Int. J. Climatol. http://dx.doi.org/10.1002/joc.3650.
Trigo, R.M., Gouveia, C.M., Barriopedro, D., 2010. The intense 2007–2009 drought in 397 the Fertile Crescent: impacts and associated atmospheric circulation. Agric. Meteorol. 150 (9), 1245–1257.
Tsakiris, G., 2017. Drought risk assessment and management. Water Resour. Manag. 31, 303–3095.
Tsakiris, G., Pangalou, D., Vangelis, H., 2007. Regional drought assessment based on the reconnaissance Drought Index (RDI). Water Resour. Manag. 21, 821–831.
Turk, M., Levin, N., Tessler, N., Saaroni, H., 2016. Recent changes and relations among drought, vegetation and wildfires in the Eastern Mediterranean: the case of Israel. Glob. Planet. Chang. 151, 28–35.
Van Loon, A.F., 2015. Hydrological drought explained. Wiley Interdiscip. Rev. Water. 2, 359–392.
Vicente-Serrano, S.M., 2006. Differences in spatial patterns of drought on different time scales: an analysis of the Iberian Peninsula. Water Resour. Manag. 20, 37–60.
Vicente-Serrano, S.M., Gonzalez-Hidalgo, J.C., de Luis, M., Raventos, J., 2004. Spatial and temporal patterns of droughts in the Mediterranean area: the Valencia region (East-Spain). Clim. Res. 26, 5–15.
Vicente-Serrano, S.M., Begueria, S., Lopez-Moreno, J.I., 2010a. A multi-scalar drought index sensitive to global warming: the standardized precipitation evapotranspiration index - SPEI. J. Clim 23, 1696–1718.
Vicente-Serrano, S.M., Begueria, S., Lopez-Moreno, J.I., Angulo, M., Kenawy, E.L., 2010b. A new global 0.58 gridded dataset (1901–2006) of a multiscalar drought index: comparison with current drought index datasets based on the Palmer drought severity index. J. Hydrometeorol. 11, 1033–1043.
Vicente-Serrano, S.M., Lasanta, T., Gracia, C., 2010c. Aridification determines changes in forest growth in Pinus halepensis forests under semiarid Mediterranean climate conditions. Agric. For. Meteorol. 150, 614–628.
Vicente-Serrano, S.M., Begueria, S. Juan, Lopez-Moreno, J.I., 2011. Comment on "Characteristics and trends in various forms of the Palmer Drought Severity Index (PDSI) during 1900-2008" by A Dai. J. Geophys. Res. Atmos. 116, D19112. http://dx.doi.org/10.1029/2011JD016410.
Vicente-Serrano, S.M., Aidel, Z., Teodoro, L., Yolanda, P., 2012. Dryness is accelerating degradation of vulnerable shrublands in semiarid Mediterranean environments. Ecol. Monogr. 82, 407–428.
Vicente-Serrano, S.M., Lopez-Moreno, J.I., Begueria, S., Lorenzo-Lacruz, J., Sanchez-Lorenzo, A., Garcia-Ruiz, J.M., Azorin-Molina, C., Moran-Tejeda, E., Revuelto, J., Trigo, R., 2014. Evidence of increasing drought severity caused by temperature rise in southern Europe. Environ. Res. Lett. 9, 1–9.
Vicente-Serrano, S.M., Cabello, D., Tomas-Burguera, M., Martin-Hernandez, N., Begueria, S., Azorin-Molina, C., Kenawy, A., 2015. Drought variability and land degradation in semiarid regions: assessment using remote sensing data and drought indices (1982–2011). Remote Sens. 7 (4), 4391–4423.
Voss, K.A., Famiglietti, J.S., Lo, M., de Linage, C., Rodell, M., Swenson, S.C., 2013. Ground water depletion in the Middle East from GRACE with implications for transboundary water management in the Tigris–Euphrates-Western Iran region. Water Resour. Res. 49, 904–914. http://dx.doi.org/10.1002/wrcr.20078.
Wang, Y., Xu, Y., Lei, C., Li, G., Han, L., Song, S., Yang, L., Deng, X., 2016. Spatio-temporal characteristics of precipitation and dryness/wetness in Yangtze River Delta, eastern China, during 1960–2012. Atmos. Res. 172 196-173.
Wang, H., Pan, Y., Chen, Y., 2017. Comparison of three drought indices and their evolutionary characteristics in the arid region of northwestern China. Atmos. Sci. Lett. 18, 132–139.
Wells, N., Goddard, S., Hayes, M.J., 2004. A self-calibrating Palmer Drought Severity Index. J. Clim. 17, 2335–2351.
WFP (World Food Program), 2014. Will drought worsen the impact of conflict on food insecurity? In: Special Focus Syria (March 2014).
White, D., Richman, M., Yarnal, B., 1991. Climate regionalization and rotation of principal components. Int. J. Climatol. 11, 1–25.
White, D., Sivakumar, M.V.K., Pulwarty, R., 2014. Managing drought risk in a changing climate: the role of national drought policy. Weather Clim. Extrem. 3, 4–13.
Wilhite, D.A., Glantz, M.H., 1985. Understanding the drought phenomenon: the role of definitions. In: Wilhite, D.A., Easterling, W.E., Wood, D.A. (Eds.), Planning for

Drought. Vestview Press, Boulder, CO, pp. 11–27.
Yu, W., Shao, M., Ren, M., Zhou, H., Jiang, H., Li, D., 2013. Analysis on spatial and temporal characteristics drought of Yunnan Province. Acta Ecol. Sin. 33 (3), 317–324.
Zambrano, F., Wardlow, B., Tadesse, T., Saaverda, M.L., Lagos, O., 2017. Evaluating satellite-derived long-term historical precipitation datasets for drought monitoring in Chile. Atmos. Res. 186, 26–42.
Zargar, A., Sadiq, R., Naser, B., Khan, F.I., 2011. A review of drought indices. Environ. Rev. 19, 333–349.
Zou, L., Xia, J., She, D., 2017. Drought characteristic analysis based on an improved PDSI in the Wei River Basin of China. Water 9, 178. http://dx.doi.org/10.3390/w9030178.